

# Solute–Solvent Complex Kinetics and Thermodynamics Probed by 2D-IR Vibrational Echo Chemical Exchange Spectroscopy

Junrong Zheng<sup>†,‡</sup> and M. D. Fayer<sup>\*,†</sup>

Department of Chemistry and Pulse Institute, Stanford University, Stanford, California 94305

Received: May 8, 2008; Revised Manuscript Received: June 12, 2008

The formation and dissociation kinetics of a series of triethylsilanol/solvent weakly hydrogen bonding complexes with enthalpies of formation ranging from  $-1.4$  to  $-3.3$  kcal/mol are measured with ultrafast two-dimensional infrared (2D IR) chemical exchange spectroscopy in liquid solutions at room temperature. The correlation between the complex enthalpies of formation and dissociation rate constants can be expressed with an equation similar to the Arrhenius equation. The experimental results are in accord with previous observations on eight phenol/solvent complexes with enthalpies of formation from  $-0.6$  to  $-2.5$  kcal/mol. It was found that the inverse of the solute–solvent complex dissociation rate constant is linearly related to  $\exp(-\Delta H_0/RT)$  where  $\Delta H_0$  is the complex enthalpy of formation. It is shown here, that the triethylsilanol–solvent complexes obey the same relationship with the identical proportionality constant, that is, all 13 points, five silanol complexes and eight phenol complexes, fall on the same line. In addition, features of 2D IR chemical exchange spectra at long reaction times (spectral diffusion complete) are explicated using the triethylsilanol systems. It is shown that the off-diagonal chemical exchange peaks have shapes that are a combination (outer product) of the absorption line shapes of the species that give rise to the diagonal peaks.

## I. Introduction

Solute–solvent intermolecular interactions can lead to well defined solute–solvent complexes.<sup>1</sup> For systems in which solute–solvent complexes exist, the solution cannot be described in terms of a simple radial distribution function<sup>2</sup> with solvent molecules moving diffusively into and out of the first solvation shell of a solute. The typical organic solute–solvent interaction energy is weak, less than 5 kcal/mol.<sup>3</sup> This value suggests that the dissociation time scale of solute–solvent complexes in room temperature solutions will be faster than 1 ns.<sup>4</sup> However, complexes that exist for even short times, ten to a hundred picoseconds, fundamentally change the behavior of a solvent surrounding a solute. It may be necessary for a solute–solvent complex to dissociate before a bimolecular reaction can occur. Therefore, understanding the dynamics of solute–solvent interactions is important for understanding the molecular level reaction mechanisms in solutions.

Because of the short time scales, measuring the kinetics of reactions with activation energy smaller than 5 kcal/mol at room temperature under thermal equilibrium conditions has proven to be difficult.<sup>4</sup> Recently nonlinear IR techniques especially 2D IR methods<sup>5–13</sup> have overcome the difficulties.<sup>14–21</sup> The techniques have an intrinsic fast temporal resolution that can be  $<100$  fs. In addition, perturbations of the dynamics using 2D-IR methods have been shown to be negligible,<sup>17</sup> and there are well defined internal tests to determine if the true equilibrium dynamics are in fact being observed.<sup>17</sup> The basic principle of the methods is to monitor the time evolution of the of the 2D-IR spectrum of a vibration with a frequency that is changed by an equilibrium chemical process. If the vibration has different frequencies for two species that are interconverting, the time

evolution of the 2D spectrum can provide a direct measurement of the rate of interconversion.

Recently we applied the 2D IR chemical exchange method<sup>15–23</sup> to the study of formation and dissociation kinetics of eight phenol–solvent complexes with enthalpies of formation from  $-0.6$  to  $-2.5$  kcal/mol under thermal equilibrium conditions at room temperature.<sup>20</sup> We found that there is a clear correlation between the enthalpies of formation of the complexes and the dissociation time constants (inverse of the dissociation rate constants), and the correlation can be described by an equation similar to the Arrhenius equation.<sup>20,21</sup> It was determined that the solute–solvent complex dissociation time constant is linearly related to  $\exp(-\Delta H^0/RT)$  where  $\Delta H^0$  is the complex enthalpy of formation,  $R$  is the gas constant, and  $T$  is the absolute temperature. This observation is interesting and important. If it is general for most weak organic solute–solvent complexes, then the dissociation kinetics of other solute–solvent complexes might be estimated based on their enthalpies of formation. Enthalpies of formation can be obtained from standard tools such as FT-IR through van't Hoff plots.<sup>24</sup> To test the generality of the observed enthalpy/kinetics correlation of the phenol/solvent systems, we studied another series of solute–solvent systems with enthalpies of formation from  $-1.4$  to  $-3.3$  kcal/mol. The vibrational probe is the OD hydroxyl stretch of triethylsilanol with the OH replaced by OD. The OD stretch has a much longer lifetime ( $\sim 160$  ps in  $\text{CCl}_4$ ) than that of the OD stretch of phenol-OD molecules ( $\sim 15$  ps in  $\text{CCl}_4$ ). The substantially longer vibrational lifetime allows us to extend the measurements to stronger complexes (enthalpies of formation more negative than  $-2.5$  kcal/mol). In addition, the longer probe lifetime provides a much longer time window in which to measure the kinetics. In previous studies, the dynamic properties of the phenol-benzene complexes were mostly derived from experiments at relatively short reaction periods (limited by the lifetimes of the probes). Therefore, spectroscopic features of 2D IR chemical exchange spectra at long time have not been

\* Corresponding author. E-mail: fayer@stanford.edu.

<sup>†</sup> Department of Chemistry, Stanford University.

<sup>‡</sup> Pulse Institute, Stanford University.

experimentally explored. The new systems offer an opportunity to examine the spectral features at long time and compare them to theoretical predictions.<sup>23</sup> It is found experimentally and theoretically that the 2D chemical exchange off-diagonal line shapes are determined by a combination of the two linear absorption line shapes. Each spectrum is taken as a vector, and the peak shapes are determined by the outer product of the two spectral vectors.

## II. Experimental Procedures

The systems are room-temperature solutions of triethylsilanol with the hydroxyl OH replaced by OD (TES) in benzene/ $\text{CCl}_4$  (TES:benzene: $\text{CCl}_4$  = 4.6:80:100, molar ratio), toluene/ $\text{CCl}_4$  (TES:toluene: $\text{CCl}_4$  = 4:69:100, molar ratio), *p*-xylene/ $\text{CCl}_4$  (TES:*p*-xylene: $\text{CCl}_4$  = 4.2:38:100, molar ratio), mesitylene/ $\text{CCl}_4$  (TES:mesitylene: $\text{CCl}_4$  = 4:34:100, molar ratio) and acetonitrile/ $\text{CCl}_4$  (TES:acetonitrile: $\text{CCl}_4$  = 3:8:100, molar ratio) mixed solvents. The low concentrations of TES make sure that vibrational excitation transfer between the TES species is negligible. In the solutions, a good portion of the TES molecules form complexes with the aromatic molecules, while other TES remain free (uncomplexed).

The free and complexed TES species are in thermal equilibrium with the complexes continually dissociating to make the free TES and the free TES continually associating to form complexes. Because the system is in equilibrium, there is no change in the overall number of the free and complexed species. Therefore, the exchange rate cannot be determined from the IR absorption spectrum of the OD stretch. The exchange rates are measured with the 2D IR exchange method,<sup>17</sup> the rotational and vibrational dynamics are measured with pump–probe experiments,<sup>18,25</sup> and the strengths of the triethylsilanol-solvent molecule complexes are measured with the temperature dependent FT-IR absorption spectrum using van't Hoff plots.<sup>21,24</sup> The OD stretch of TES has a very long vibrational lifetime that makes it possible to measure the exchange at long reaction periods. In  $\text{CCl}_4$  TES exists only as the free species and has a lifetime of 160 ps. The lifetimes of the complexes are shorter, but still many tens of picoseconds.

Details of the experimental method used for these 2D IR chemical exchange experiments have been described previously.<sup>18,22,26,27</sup> Very briefly, in a 2D IR vibrational echo chemical exchange experiment, three ultrashort IR pulses tuned to the frequency range of the vibrational modes of interest are crossed in the sample. Because the pulses are very short, they have a broad frequency bandwidth that makes it possible to simultaneously excite a number of vibrational modes. The first laser pulse “labels” the initial structures of the species by establishing their initial frequencies,  $\omega_\tau$ . The second pulse ends the first time period  $\tau$  and starts clocking the reaction time period  $T_w$  during which the labeled species undergo chemical exchange, that is, complexes formation and dissociation. The chemical exchange will be manifested in the 2D spectrum by growth of off-diagonal peaks if the exchange changes the vibrational frequency of the vibrational mode under study. In addition to chemical exchange, vibrational relaxation to the ground-state and orientational relaxation will influence the 2D spectrum. The third pulse ends the population period of length  $T_w$  and begins a third period of length  $\leq \tau$ , which ends with the emission of the vibrational echo pulse of frequency  $\omega_m$ , which is the signal in the experiment. The vibrational echo signal reads out information about the final structures of all labeled species by their frequencies,  $\omega_m$ . During the period  $T_w$  between pulses 2 and 3, chemical exchange occurs when two species in equilib-

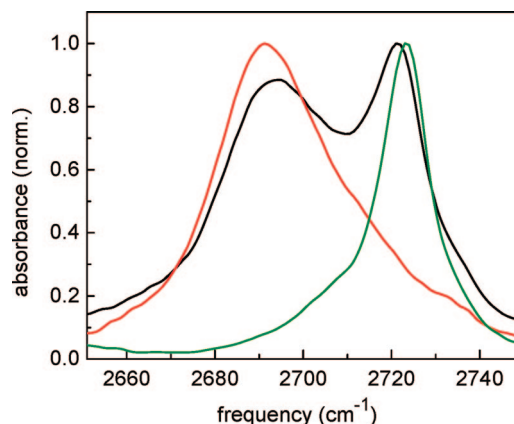


**Figure 1.** FT-IR absorption spectra of the OD stretch of triethylsilanol (TES, hydroxyl H replaced with D) in  $\text{CCl}_4$  (free TES, green curve), TES in benzene (TES–benzene complex, red curve), and TES in the mixed benzene/ $\text{CCl}_4$  solvent, which displays absorptions for both free and complexed TES (black curve).

rium interconvert without changing the overall number of either species. The exchange causes new off-diagonal peaks to grow in as  $T_w$  is increased. The growth of the off-diagonal peaks in the 2D IR spectra with increasing  $T_w$  is used to extract the dissociation and formation time constants of the complexes. The dissociation time constant,  $\tau_d$ , is the inverse of the dissociation rate constants,  $k_d$ . The rates of dissociation and formation are equal because the system is in equilibrium.<sup>17</sup>

The vibrational population relaxation time constants and orientational relaxation time constants were measured with the polarization selective IR pump–probe experiments.<sup>18,28</sup> The orientational relaxation time constants, obtained in pure solvents, were corrected for the solvent viscosity differences between the pure aromatic solvent or  $\text{CCl}_4$  and the mixed solvents used in the chemical exchange experiments using the Debye–Stokes–Einstein equation. Viscosity measurements were made with Cannon Ubbelohde Viscometers at 24 °C, the same temperature used for the vibrational echo and pump–probe measurements.

The enthalpies of formation of the solute–solvent complexes were determined by measuring the temperature dependence of the equilibrium constants with FT-IR. The temperature range was 25–65 °C.<sup>20,21</sup>

## III. Results and Discussion

**A. Chemical Exchange Dynamics.** When TES molecules are dissolved in a benzene/ $\text{CCl}_4$  mixture, some of the TES form complexes with benzene, while others remain free (not complexed). Experimental evidence for the formation of triethylsilanol/benzene complexes is the shift of the OD stretch frequency of TES to a lower frequency in benzene compared to that of TES in  $\text{CCl}_4$ . Figure 1 shows FT-IR spectra of triethylsilanol-OD in pure  $\text{CCl}_4$ , in pure benzene, and a mixed benzene/ $\text{CCl}_4$  solvent. When TES is dissolved in  $\text{CCl}_4$ , no hydrogen bond is formed between the solute and solvent molecules. The OD stretch frequency is at 2723  $\text{cm}^{-1}$ . The peak is relatively narrow, and the full width at half-maximum (fwhm) is 14  $\text{cm}^{-1}$ . When TES is dissolved in benzene, a  $\pi$  hydrogen bonded complex is formed between a solute and a solvent molecule. The OD stretch frequency red-shifts to 2691  $\text{cm}^{-1}$  and the fwhm becomes 25  $\text{cm}^{-1}$ . In the mixed benzene/ $\text{CCl}_4$  solvent (black curve in Figure 1), both the complexed and free species are present. The relative concentration ratio of the two species can be adjusted by changing the benzene/ $\text{CCl}_4$  ratio.

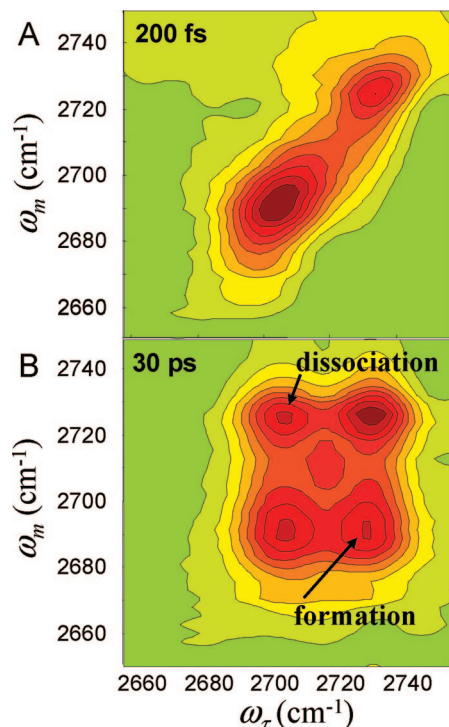


**Figure 2.** 2D-IR vibrational echo spectra of the OD stretch of TES in the mixed benzene/ $\text{CCl}_4$  solvent. The data have been normalized to the largest peak for each  $T_w$ . Each contour represents 10% change in amplitude. (A) Data for  $T_w = 200$  fs. There are only peaks on the diagonal because chemical exchange has yet to occur. (B) Data for  $T_w = 30$  ps. At the longer time, additional peaks have grown in because of chemical exchange, that is, the formation and dissociation of the complex of TES and benzene.

At room temperature, the two species of TES are under dynamic equilibrium in the mixed solution. The complexed and free species are constantly exchanging. The TES/benzene complex enthalpy of formation ( $\Delta H^0$ ) in the solution was determined to be  $-1.4$  kcal/mol. On the basis of our previous work on phenol/benzene complexes and other phenol/substituted benzene complexes in the same types of mixed solvents, this  $\Delta H^0$  value suggests that the exchange reactions will be very fast.

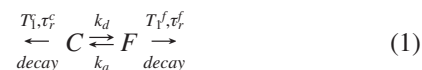
Figure 2 displays two 2D IR spectra (only the 0–1 transition region is shown) of TES in a benzene/ $\text{CCl}_4$  mixture for a very short ( $T_w = 200$  fs) and a long ( $T_w = 30$  ps) reaction period. For the very short reaction time no chemical exchange has occurred. The species (complexed or free TES molecules) in the sample are unchanged. Therefore, in the 2D IR spectrum, the  $\omega_\tau$  frequency (initial frequency) and the  $\omega_m$  frequency (final frequency) for each peak are unchanged. Only two peaks are present in the spectrum, and they are on the diagonal. These peaks correspond to the absorption bands shown in Figure 1 for the mixed solvent. For the long period, considerable exchange has occurred. During the 30 ps  $T_w$  period, some of the complexes that existed at the beginning of the period have dissociated to become free. Some of the free TES have associated with benzenes to become complexes. Two off-diagonal peaks have grown in. The off-diagonal peaks originate from the exchange reactions. The peak labeled as “dissociation” has its  $\omega_\tau$  (initial frequency) at the lower frequency, showing that the initial structure was complexed TES. Its  $\omega_m$  (final frequency) is the higher frequency, which shows the final structure is free TES. This off-diagonal peak arises from those free TES molecules formed from initially complexed molecules.

The “formation” peak (at 30 ps) arises from complexed TES molecules that were initially free species. The two diagonal peaks are the result of molecules that have either not exchanged or have exchanged an even number of times during the 30 ps reaction period so that they are the same species at the end of the reaction period as they were initially.

The  $T_w$  dependent growth of the off-diagonal peaks provides direct information on the time dependence of the formation and dissociation of the TES-benzene complex. As shown in Figure 2A, at very short time there are no off-diagonal peaks. As  $T_w$  increases, the off-diagonal peaks increase in amplitude. By 30 ps (Figure 2B) they are substantial. Illustrations of the growth of the off-diagonal peaks as chemical exchange proceeds have been given previously.<sup>17–19,21</sup> The exchange kinetics can be extracted from analyzing the time dependent peak volumes.<sup>17,21,22</sup> If spectral diffusion is fast compared to the chemical exchange rate, the peak intensities can be used to obtain the chemical exchange dynamics.<sup>17,21</sup>

The 2D IR signal is affected by four dynamic processes: chemical exchange, vibrational relaxation of the OD stretch excitation, orientational relaxation of the species, and the spectral diffusion.<sup>29,30</sup> Chemical exchange causes the two off-diagonal peaks to grow in and the two diagonal peaks shrink. Vibrational relaxation causes all four peaks to decrease in amplitude. Orientational relaxation randomizes the anisotropy of the excited molecules induced by the polarized laser pulses, which reduces all four peaks. Spectral diffusion is the result of time dependent interactions of the vibrational transition with the solvent. Interactions of the vibrational oscillator (OD stretch) cause its transition frequency to evolve. At sufficiently long time, all oscillators will have sampled all frequencies that give rise to the absorption line shape. In the 2D-IR vibrational echo spectrum, at short time the diagonal peaks are elongated along the diagonal, which reflects inhomogeneous broadening of the system. At sufficiently long  $T_w$ , all possible solvent configurations have been sampled, and the dynamic line width is equal to the absorption line width. In a 2D spectrum complete spectral diffusion is manifested by a change in the diagonal 2D line shapes from elongated along the diagonal to symmetrical about the diagonal. From the data, it was determined that spectral diffusion is complete by  $\sim 4$  ps. Spectral diffusion changes the shapes of the peaks but preserves their volumes. Therefore, if the volume of the peaks is used in determining the chemical exchange kinetics, spectral diffusion drops out of the problem.<sup>17,22</sup> In addition, the magnitude of signal of each peak is determined by the transition dipole moments of the species.<sup>31</sup> The diagonal peaks have amplitudes proportional to  $\mu_i^4$ , where  $i$  labels the species, free and complex. The off-diagonal peaks depend on the transition dipoles of both species as  $\mu_i^2 \mu_j^2$ .

By taking into account all of these factors, a kinetic model was constructed to analyze the exchange kinetics.<sup>17,18,21,22</sup> The model is illustrated schematically as



where the complexed (C) and free (F) species can undergo chemical exchange with dissociation and association rate constants,  $k_d$  and  $k_a$ , respectively. The free and complex species decay due to vibrational relaxation with time constants  $T_1^f$  and  $T_1^c$ , respectively, and the species undergo orientational relaxation with time constants  $\tau_r^f$  and  $\tau_r^c$ , respectively. The lifetime and orientational relaxation time constants are obtained from pump–probe experiments, the reaction time ( $T_w$ ) dependent species’ concentrations are provided by the 2D IR measurements

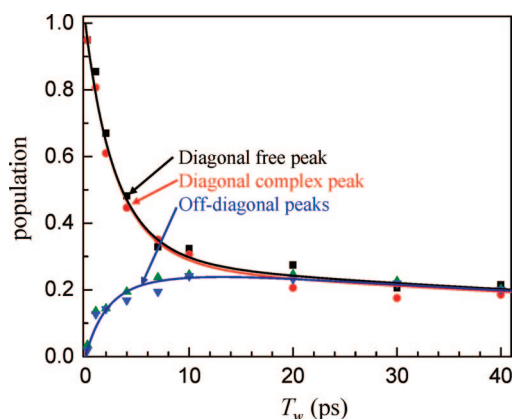


**Figure 3.**  $T_w$  dependent data (symbols) showing the time dependence of the diagonal and off-diagonal chemical exchange peaks, in the 2D IR vibrational echo spectra. The solid lines through the data are the result of the single adjustable parameter fit that yields the TES/benzene dissociation time constant,  $\tau_d = 9$  ps.

after appropriate scaling with the transition dipole moments, and the ratio of the dissociation and association rate constants is determined using the equilibrium constant  $K$  obtained from FT-IR measurements.<sup>17,21</sup> Therefore, there is only one adjustable parameter,  $\tau_d = 1/k_d$ , necessary to fit the experimental data.

The kinetics of the formation and dissociation of TES/benzene complexes were analyzed with the model outlined above and described in more detail previously.<sup>17,21,22</sup> The input parameters used to implement the model shown in equation 1 are  $T_1^f = 95$  ps,  $T_1^i = 160$  ps,  $\tau_c^r = 2.8$  ps,  $\tau_r^f = 3.2$  ps, and the ratio of the complexed and free triethylsilanol concentrations [complex]/[free] = 1. The ratio of the square of the transition dipole moments is  $\mu_c^2/\mu_f^2 = 1.71$ .

Figure 3 displays the  $T_w$  dependent populations associated with the four peaks shown at 30 ps in Figure 2B. The diagonal peaks decay. The off-diagonal peaks grow in and then decay. Because the system is in equilibrium, the rates of formation and dissociation of the complexes are equal, and the off-diagonal peaks grow in with the same time dependence.<sup>17</sup> The solid lines through the data are calculated with the single adjustable parameter, the dissociation time constant,  $\tau_d$ . The agreement between the fit and the data is quite good. The results give the dissociation time constant for the TES/benzene complex,  $\tau_d = 9$  ps.

The analysis of the TES/benzene data has been described in some detail. We now wish to compare the complex dissociation time obtained for the TES-benzene complex with the other four TES complexes studied here. We will then combine the new results for the five TES complexes with previous results obtained on eight complexes involving the solute phenol rather than TES to investigate the trend in the dissociation times as a function of the enthalpies of formation of the 13 complexes.

The analysis used for the TES/benzene system and the TES/acetonitrile system is identical to that employed previously for phenol/benzene and seven other systems.<sup>20,21</sup> However, in contrast to the other systems studied here and previously, the pump-probe population relaxation decays of the OD stretch of the TES molecules in the pure solvents toluene, *p*-xylene and mesitylene are biexponentials rather than single exponentials. The precise reason for the biexponential population decay is unknown. However, the spectra of the solvents give an indication of the mechanism. Figure 4 shows the spectra of all five solvents. Benzene and acetonitrile show no absorption in the region of the OD stretch absorption (see Figure 1). In

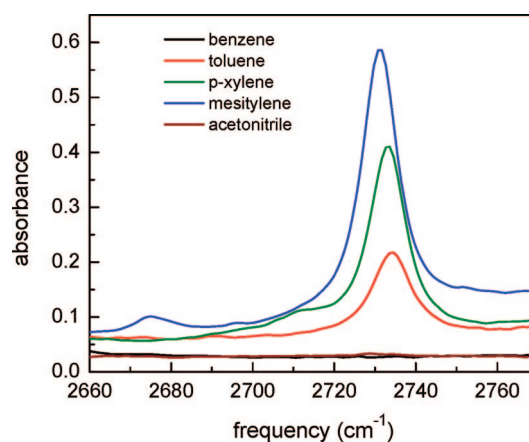


**Figure 4.** FT-IR spectra of pure acetonitrile, benzene, toluene, *p*-xylene, mesitylene in the region where the OD stretch of TES absorbs. A peak is apparent in toluene, *p*-xylene, and mesitylene at  $\sim 2730$   $\text{cm}^{-1}$  but not in benzene or acetonitrile.

contrast, toluene, *p*-xylene, and mesitylene all have absorptions in the OD stretch region. The absorbance increases as the number of methyl groups increases. The ratio of the optical densities of this peak of the three molecules is  $\sim 1:2:3$  (toluene: *p*-xylene:mesitylene), very close to the ratio of the number of the methyl groups. Therefore, it is reasonable to assume that the absorbance is a result of a combination band or overtone involving the methyl group. The proximity of the solvent mode frequency to the frequency of the OD stretch of both the complex and free species can provide a pathway for vibrational population decay that involves relaxation directly into these solvent degrees of freedom involving the methyl groups.<sup>32,33</sup> The biexponential decay could arise because only a fraction of the TES are in a configuration relative to the aromatic solvent molecule that permits the solvent pathway to be active.

The biexponential decay can be readily incorporated into the chemical exchange kinetic analysis. The 2D IR kinetic analysis can be separated into two independent single exponential parts. The ratio of the two parts is determined by the prefactors (coefficients) of the biexponential. For each single exponential part the model used above and previously is applied.<sup>17,21</sup> Pump-probe measurements on TES in toluene, *p*-xylene, and mesitylene yield the biexponential complex lifetimes and amplitudes (see Table 1 for values), but TES in  $\text{CCl}_4$  is a single exponential.

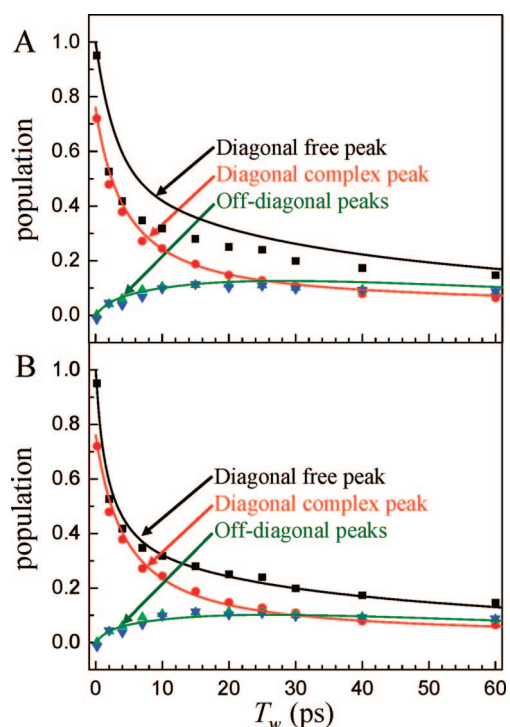
In the analysis performed above and previously,<sup>21</sup> the lifetime for the complex is the lifetime measured in the pure complexing solvent, and the lifetime for the free species is the lifetime measured in  $\text{CCl}_4$ . Figure 5A shows the results of fitting the  $T_w$  dependent 2D IR spectra for the TES/mesitylene- $\text{CCl}_4$  system using the model in which the complex has the measured biexponential population relaxation but the free species decays as a single exponential. The analysis yields the only adjustable parameter,  $\tau_d = 28$  ps. As seen in Figure 5A, the model does a good job in fitting the TES/mesitylene complex diagonal peak and the two off-diagonal peaks, but it does not reproduce the free diagonal peak very well. The experimental data decay much faster than the best fit. A reasonable explanation for this is that the vibrational population relaxation of the free species in the mixed solvent containing aromatics with methyl groups is biexponential.

Figure 5B shows that same data fit again, but this time taking the population decay of both the free TES and the complex to be biexponential. In this fit there are three adjustable parameters,  $\tau_d$  and the amplitude and decay time of the fast component of

TABLE 1: Experimentally Determined Parameters<sup>a</sup>

sample	$\tau_d$ (ps)	$\Delta H^0$ (kcal/mol)	$T_1$ (ps)	$A$	$\tau_r^f$ (ps)	$\tau_r^c$ (ps)	$\tau_r^{cp}$ (ps)
TES			160	1	3.2	3.2	3.2
TES/BZ	9 ± 2	-1.4	95	1	3.3	2.8	3.3
TES/TL	11 ± 2	-1.6	95 (1)	0.92 (0.08)	3.2	3.8	4.2
TES/pX	18 ± 3	-2.1	101 (1.2)	0.87 (0.13)	3.3	4.1	5.1
TES/MS	26 ± 5	-2.4	61 (2.8)	0.80 (0.20)	3.3	6.9	8.7
TES/AN	140 ± 20	-3.3	22	1	3.0	8.5	7

<sup>a</sup> Samples: TES, TES in CCl<sub>4</sub>; TES/BZ, TES in benzene/CCl<sub>4</sub>; TES/TL, TES in toluene/CCl<sub>4</sub>; TES/pX, TES in *p*-xylene/CCl<sub>4</sub>; TES/MS, TES in mesitylene/CCl<sub>4</sub>; TES/AN, TES in acetonitrile/CCl<sub>4</sub>.  $\tau_d$ : complex dissociation time constant.  $\Delta H^0$ : complex enthalpy of formation.  $T_1$ : population decay time of free TES (160 ps) and TES complexes. For bi-exponential decays, the fast component is given in parentheses.  $A$ : normalized amplitude of population decay. For bi-exponential decays, the amplitude of the fast component is given in parentheses.  $\tau_r^f$ : orientational relaxation time constant of the free species in the mixed solvent.  $\tau_r^c$ : orientational relaxation time constant of the complex in the mixed solvent.  $\tau_r^{cp}$ : orientational relaxation time constant of the complex in the pure complexing solvent.



**Figure 5.**  $T_w$  dependent data (symbols) showing the time dependence of the diagonal and off-diagonal 2D IR vibrational echo chemical exchange peaks for the TES/mesitylene–CCl<sub>4</sub> system. The solid curves are from fits to the data. (A) Solid curves are the fitting results for the model in which the OD stretch population of the complex decays as a biexponential as measured on TES in pure mesitylene, but the OD stretch population decay of the free species is a single exponential. The data are fit with one adjustable parameter,  $\tau_d$ . The fit yields  $\tau_d = 28$  ps. The fit misses the free diagonal peak data but is quite good for the other three peaks. (B) Solid curves are the fitting results for the model in which both the complexed and free TES have biexponential population decays. The fit is substantially improved and yields  $\tau_d = 23$  ps.

the population decay of the free TES in the mesitylene–CCl<sub>4</sub> solvent. As can be seen in Figure 5B, the fit is much better, but there are more adjustable parameters. The results yield  $\tau_d = 23$  ps. This value is quite similar to the value obtained from the fitting shown in Figure 5A, indicating that the value obtained for  $\tau_d$  is robust. The  $\tau_d$  value is mainly determined by the growth of the off-diagonal peaks. For the three solvents that display

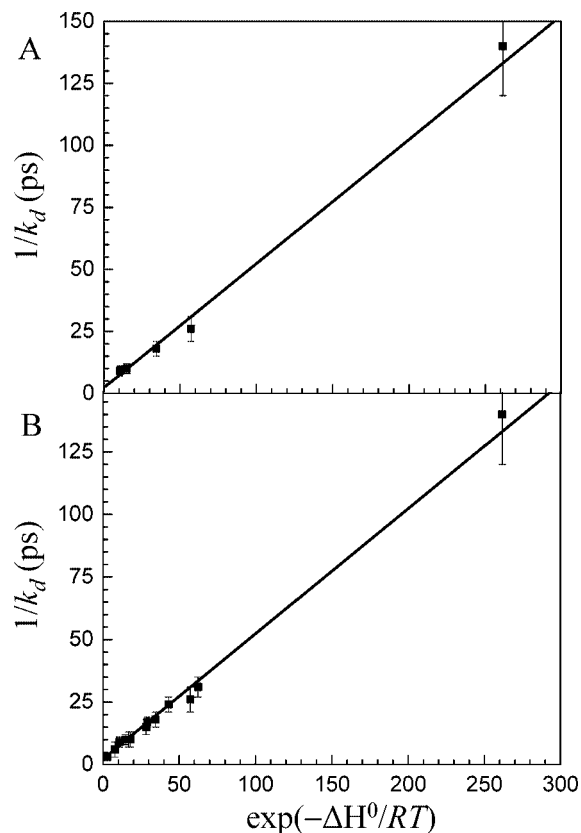


**Figure 6.** Dissociation times of the complexes,  $\tau_d$  ( $1/k_d$ ), plotted vs  $\exp(-\Delta H^0/RT)$  where  $\Delta H^0$  is the enthalpy of formation of the solute–solvent complex. The line through the data is given by equation 2. (A) Data from the five triethylsilanol systems measured here. (B) Data from the five triethylsilanol systems and from the eight phenol systems measured previously.<sup>17,21</sup> The same relation (eq 2) holds for all 13 data points.

the biexponential population decays, we fit the data both ways, that is, the free TES population relaxation is single or biexponential. The  $\tau_d$  values are taken as the average of the two values. So for TES/mesitylene we obtain  $\tau_d = 26 \pm 5$  ps. The  $\tau_d$  values for the five systems studied are given in Table 1.

#### B. Correlation between Kinetics and Thermodynamics.

Figure 6A shows the correlation between the dissociation time constant  $\tau_d$  ( $1/k_d$ ) and  $\exp(-\Delta H^0/RT)$ , where  $\Delta H^0$  is the enthalpy of the formation of the complex. The data fall on a line within experimental error. This is the same behavior that was found previously for the eight complexes of phenol–OD. Figure 6B shows the five data points for the TES complexes and the eight data points for the phenol complexes. The line through the data in both panels is

$$1/k_d = B + A^{-1} \exp(-\Delta H^0/RT) \quad (2)$$

where  $B = 2.3$  ps and  $A^{-1} = 0.5$  ps are constants. All of the data fall on the same line. The results demonstrate again that there is a clear correlation between the dissociation time constant and the enthalpy of formation of the complexes. The deviation from an intercept of 0, that is the fact that  $B = 2.3$  ps, could arise for a number of reasons. Previously we suggested that even in the limit that  $\Delta H^0$  goes to zero, a finite time will be required for the pseudocomplex (no binding) to separate.<sup>21</sup> A simple calculation showed that the intercept is the right time scale for diffusive separation.<sup>21</sup> Another possibility could be a systematic error in the determination of the  $\Delta H^0$  values, which were obtained with the assumption that the enthalpies and

entropies of formation are temperature independent over the temperature range used to determine them.

The important feature of Figure 6B is that all of the data fall on the same line. Transition state theory<sup>24</sup> would suggest that  $k_d$  should depend on the activation free energy,  $\Delta G^*$ , not on the enthalpy of formation,  $\Delta H^0$ . In terms of simple transition state theory, the dissociation rate constant can be written as

$$k_d = \frac{k_B T}{h} e^{-\Delta G^*/RT} = \frac{k_B T}{h} e^{\Delta S^*/R} e^{-\Delta H^*/RT} \quad (3)$$

where  $\Delta G^*$  is the activation free energy,  $\Delta S^*$  is the activation entropy, and  $\Delta H^*$  is the activation enthalpy. If the activation enthalpy is proportional to the dissociation enthalpy,  $\Delta H^* \propto \Delta H^0$ , and the activation entropy  $\Delta S^*$  is essentially a constant, independent of the molecular structure of the complexes and differences in the solvents, then equation 2 and the behavior displayed in Figure 6 are obtained.

The data in Figure 6B has eight complexes of phenol and phenol derivatives with various substituted benzenes<sup>21</sup> and five complexes of triethylsilanol with substituted benzenes and acetonitrile. All of the complexes involve a hydrogen bond with a hydroxyl. However, the complexes vary significantly in their molecular structure. It is not clear how general the correlation between the complex dissociation time and the enthalpy of formation is for other complexes that do not involve a hydrogen bond to a hydroxyl. Nonetheless, equation 2 may serve as a guide for estimating the dissociation times of complexes.

**C. 2D IR Chemical Exchange Line Shapes.** The long vibrational lifetimes of the OD stretch of both the free (~160 ps) and complexed TES molecules (see Table 1) allow 2D IR vibrational echo chemical exchange data to be acquired at long reaction times ( $T_w$ ). The data for long reaction periods reveal an important feature of the 2D IR chemical exchange spectra that has not been previously explicated. If  $T_w$  is sufficiently long the 2D line shapes are combinations, the outer products, of the linear absorption line shapes of the two exchanging species.

At short  $T_w$ , spectral diffusion causes the diagonal 2D line shapes to change with time. At sufficiently long time, spectral diffusion is complete, and the line shapes obtain their long time limit. It has been argued that the off-diagonal peaks generated by chemical exchange are always effectively in the long  $T_w$  limit because the frequencies within the inhomogeneous lines of the exchanging species are uncorrelated, and, therefore, the exchange process itself cause complete spectral diffusion.<sup>22</sup> Even if there is frequency correlation in the exchange, at long  $T_w$  when spectral diffusion is complete, the diagonal and off-diagonal peaks will no longer change shape with increasing  $T_w$ . In the long  $T_w$  limit, theory predicts that the line shapes of the off-diagonal peaks can be expressed as,<sup>23</sup>

$$S(\omega_\tau, T_w, \omega_m) \propto W_A(\omega_\tau) \otimes W_B(\omega_m) \quad (4)$$

where  $S(\omega_\tau, T_w, \omega_m)$  is the off-diagonal exchange peak signal and  $\otimes$  is the outer product between the two vectors,  $W_A(\omega_\tau)$  and  $W_B(\omega_m)$ .  $W_A(\omega_\tau)$  is the vector composed of the linear absorption spectrum, that is the intensity at each frequency, of species A, which is initially excited by pulse 1, and  $W_B(\omega_m)$  is the vector composed of the linear absorption spectrum of species B, which is the species that emits the vibrational echo following pulse 3. For the diagonal peaks, the signal is proportional to  $W_A(\omega_\tau) \otimes W_A(\omega_m)$  and  $W_B(\omega_\tau) \otimes W_B(\omega_m)$ .

According to theory at long  $T_w$  when spectral diffusion is complete, the line shapes of the diagonal peaks are symmetric about the two axes. The line shapes of the off-diagonal chemical exchange peaks will not be symmetric if the two exchanging

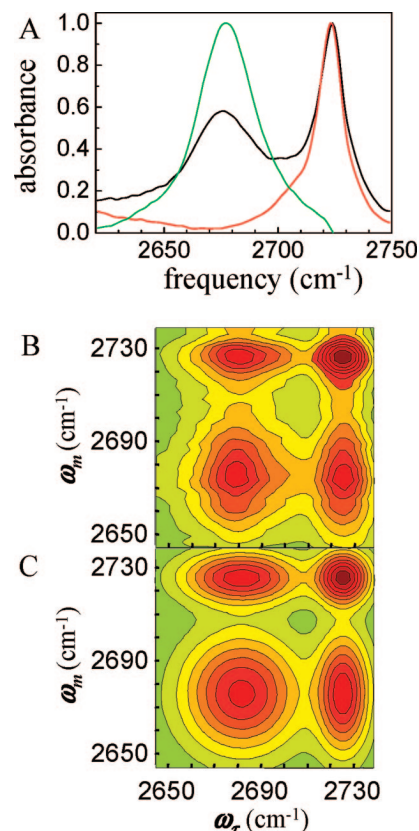


**Figure 7.** (A) FT-IR absorption spectra of the OD stretch of TES in  $\text{CCl}_4$  (free TES, green curve), TES in mesitylene (TES/mesitylene complex, red curve), and TES in the mixed mesitylene/ $\text{CCl}_4$  solvent, which displays absorptions for both free and complexed TES (black curve). (B) Experimental 2D IR spectrum ( $T_w = 60$  ps) of TES in the mixed mesitylene/ $\text{CCl}_4$  solvent. The off-diagonal peaks have the highly asymmetric shapes predicted by equation 4. (C) Calculated 2D IR spectrum using the absorption line shapes as input in accord with equation 4. The calculation reproduces the asymmetric line shapes of the off-diagonal peaks very well. Each contour is a 10% change in amplitude.

species have different absorption line shapes. A very clear example of this behavior is displayed by the 2D IR vibrational echo chemical exchange spectrum of the TES/mesitylene- $\text{CCl}_4$  system. Figure 7 displays the linear absorption spectrum (A), the 2D IR spectrum at 60 ps, which is in the long  $T_w$  limit (B), and the calculated spectrum (C). In the TES/mesitylene system, in the absorption spectrum (A) the complex peak is  $34 \text{ cm}^{-1}$  fwhm, the free peak is  $14 \text{ cm}^{-1}$  fwhm, and the two peaks are separated by  $46 \text{ cm}^{-1}$ . The substantial difference in the two linewidths and the large separation of the peaks makes it possible to cleanly observe the behavior in the 2D spectrum.

The 2D IR spectrum shown in Figure 7B displays the behavior embodied in equation 4. The off-diagonal dissociation peak (upper left-hand peak) is broad along the  $\omega_\tau$  axis and narrow along the  $\omega_m$  axis. The off-diagonal dissociation peak comes from complexes at the time of the first pulse ( $\omega_\tau$  axis), which have a broad spectrum, and free species at the time of echo emission ( $\omega_m$  axis), which have a narrow spectrum. The formation peak (lower right-hand peak) is narrow along the  $\omega_\tau$  axis and broad along the  $\omega_m$  axis. The off-diagonal formation peak comes from free species at the time of the first pulse ( $\omega_\tau$  axis), which have a narrow spectrum, and complexes at the time of echo emission ( $\omega_m$  axis), which have a broad spectrum. The predictions of equation 4 were tested quantitatively as shown in Figure 7C. The linear spectrum of the TES/mesitylene- $\text{CCl}_4$

system (black curve in Figure 7A) was fit with two Gaussians. These became the two vectors,  $W_A(\omega_\tau)$  and  $W_B(\omega_m)$  in equation 4. As can be seen in Figure 7C, the calculation does an excellent job of reproducing the experimental 2D spectrum shown in Figure 7B.

#### IV. Concluding Remarks

The formation and dissociation kinetics of five triethylsilanol solute–solvent complexes at room temperature were investigated with 2D IR vibrational echo chemical exchange spectroscopy. The time dependences of the formation and dissociation of the complexes were measured by observing the growth of the off-diagonal chemical exchange peaks in the 2D IR spectrum. The dissociation time constants range from 9 to 140 ps, and were shown to be directly related to the enthalpy of formation of the complexes. The experiments are in accord with the previous observation from eight phenol/solvent complexes.<sup>17,21</sup> The correlation between the complex enthalpies of formation and dissociation rate constants for all 13 complexes, the five studied here and eight studied previously, can be expressed with an equation similar to the Arrhenius equation.<sup>21</sup>

In addition to the dynamics, theoretical predictions of the shapes of the peaks in the 2D IR chemical exchange spectrum were tested. It was demonstrated that in the long time limit, in which spectral diffusion is complete and the peaks no longer change shape, the shapes of the off-diagonal chemical exchange peaks can be highly asymmetric. The off-diagonal peaks have shapes determined by the outer product of the absorption spectra of the species that give rise to the chemical exchange spectrum.

Organic solute–solvent complexes that have dissociation time constants in the range of 10–100 ps may be quite general. In future publications, experiments will be presented that examine the solute–solvent complex dynamics of the solute chloroform with acetone and dimethyl sulfoxide and a system in which a solute can migrate to different positions on a solvent molecule.

**Acknowledgment.** This work was supported by the Air Force Office of Scientific Research (F49620-01-1-0018) and by the National Science Foundation (DMR 0652232). J.Z. thanks Pulse Institute funded by the Stanford University Dean of Research for a post-doctoral fellowship and the Stanford Graduate fellowship program for a fellowship.

#### References and Notes

- (1) Vinogradov, S. N.; Linnell, R. H. *Hydrogen Bonding*; Van Nostrand Reinhold Company: New York, 1971.
- (2) Throop, G. J.; Bearman, R. J. *J. Chem. Phys.* **1965**, *42*, 2408.
- (3) Fuchs, R.; Peacock, L. A.; Stephenson, W. K. *Can. J. Chem.* **1982**, *60*, 1953.
- (4) Frei, H.; Pimentel, G. C. *Annu. Rev. Phys. Chem.* **1985**, *36*, 491.
- (5) Asplund, M. C.; Zanni, M. T.; Hochstrasser, R. M. *Proc. Natl. Acad. Sci. USA* **2000**, *97*, 8219.
- (6) Khalil, M.; Demirdoven, N.; Tokmakoff, A. *Phys. Rev. Lett.* **2003**, *90*, 047401. (4)
- (7) Khalil, M.; Demirdoven, N.; Tokmakoff, A. *J. Phys. Chem. A* **2003**, *107*, 5258.
- (8) Asbury, J. B.; Steinel, T.; Stromberg, C.; Gaffney, K. J.; Piletic, I. R.; Goun, A.; Fayer, M. D. *Phys. Rev. Lett.* **2003**, *91*, 237402.
- (9) Steinel, T.; Asbury, J. B.; Corcelli, S. A.; Lawrence, C. P.; Skinner, J. L.; Fayer, M. D. *Chem. Phys. Lett.* **2004**, *386*, 295.
- (10) Mukherjee, P.; Kass, I.; Arkin, I.; Zanni, M. T. *Proc. Natl. Acad. Sci. U.S.A.* **2006**, *103*, 3528.
- (11) Maekawa, H. T. C.; Moretto, A.; Broxterman, Q. B.; Ge, N. H. *J. Phys. Chem. B* **2006**, *110*, 5834.
- (12) Naraharisetty, S. R. G.; Kasyanenko, V. M.; Rubtsov, I. V. *J. Chem. Phys.* **2008**, *128*, 104502.
- (13) Nee, M. J.; McCanne, R.; Kubarych, K. J.; Joffe, M. *Opt. Lett.* **2007**, *32*, 713.
- (14) Arrivo, S. M.; Heilweil, E. J. *J. Phys. Chem.* **1996**, *100*, 11975.
- (15) Kim, Y. S.; Hochstrasser, R. M. *Proc. Natl. Acad. Sci. U.S.A.* **2005**, *102*, 11185.
- (16) Woutersen, S.; Mu, Y.; Stock, G.; Hamm, P. *Chem. Phys.* **2001**, *266*, 137.
- (17) Zheng, J.; Kwak, K.; Asbury, J. B.; Chen, X.; Piletic, I.; Fayer, M. D. *Science* **2005**, *309*, 1338.
- (18) Zheng, J.; Kwak, K.; Chen, X.; Asbury, J. B.; Fayer, M. D. *J. Am. Chem. Soc.* **2006**, *128*, 2977.
- (19) Zheng, J.; Kwak, K.; Xie, J.; Fayer, M. D. *Science* **2006**, *313*, 1951.
- (20) Zheng, J.; Kwak, K.; Fayer, M. D. *Acc. Chem. Res.* **2007**, *40*, 75.
- (21) Zheng, J.; Fayer, M. D. *J. Am. Chem. Soc.* **2007**, *129*, 4328.
- (22) Kwak, K.; Zheng, J.; Cang, H.; Fayer, M. D. *J. Phys. Chem. B* **2006**, *110*, 19998.
- (23) Sanda, F.; Mukamel, S. *J. Chem. Phys.* **2006**, *125*, 014507.
- (24) Chang, R. *Physical Chemistry for the Chemical and Biological Sciences*; University Science Books: Sausalito, CA, 2000.
- (25) Tan, H.-S.; Piletic, I. R.; Fayer, M. D. *J.O.S.A. B* **2005**, *22*, 2009.
- (26) Asbury, J. B.; Steinel, T.; Fayer, M. D. *J. Lumin.* **2004**, *107*, 271.
- (27) Park, S.; Kwak, K.; Fayer, M. D. *Laser Phys. Lett.* **2007**, *4*, 704.
- (28) Tan, H.-S.; Piletic, I. R.; Fayer, M. D. *J. Chem. Phys.* **2005**, *122*, 174501. (9)
- (29) Bai, Y. S.; Fayer, M. D. *Phys. Rev. B* **1989**, *39*, 11066.
- (30) Walsh, C. A.; Berg, M.; Narasimhan, L. R.; Fayer, M. D. *Chem. Phys. Lett.* **1986**, *130*, 6.
- (31) Mukamel, S. *Principles of Nonlinear Optical Spectroscopy*; Oxford University Press: New York, 1995.
- (32) Oxtoby, D. W. *Adv. Chem. Phys.* **1981**, *47*, 487.
- (33) Kenkre, V. M.; Tokmakoff, A.; Fayer, M. D. *J. Chem. Phys.* **1994**, *101*, 10618.